CrystEngComm

Quantum Chemical Analysis of Noncovalent Bonds within Crystals. Concepts and Concerns

Journal:	*CrystEngComm*
Manuscript ID	CE-HIG-07-2023-000708.R1
Article Type:	Highlight
Date Submitted by the Author:	23-Aug-2023
Complete List of Authors:	Scheiner, Steve; Utah State University, Department of Chemistry and Biochemistry

Quantum Chemical Analysis of Noncovalent Bonds within Crystals. Concepts and Concerns

Steve Scheiner*

Department of Chemistry and Biochemistry
Utah State University
Logan, Utah 84322-0300
USA

*email: steve.scheiner@usu.edu

Abstract

While it may seem straightforward to enlist quantum chemical calculations to evaluate the energy of a particular atom-to-atom noncovalent bond within the context of a crystal structure, there are in fact a number of complicating issues that must be understood and dealt with. In addition to the primary bond of interest, the two units will typically be held together as well by secondary interactions, such as H-bonds or π··π stacking. Deletion of the groups involved in these secondary bonds perturb the electronic structure of the primary centers. There are also nonspecific interactions that span the breadth of the subunits, such as delocalized electrostatic forces and dispersion. It is important as well to consider how crystal packing forces modify the preferred geometry of not only the two subunits of primary interest but of the entire cluster.

Keywords: halogen bond; pnicogen bond; chalcogen bond; tetrel bond; H-bond; AIM; anion-anion interaction

INTRODUCTION

The ab initio design of a crystal with a desired structure via crystal engineering is a monumental task as it is predicated on a thorough understanding of all the forces between the composite units, as well as overall issues of crystal packing. When ensconced within a crystal lattice, a given molecule is surrounded by other units, whether a replica of itself or a different species entirely. There are a host of different sorts of forces that hold the molecule in its place, both attractive and repulsive. Some of the attractive forces are fairly nonspecific, such as the overall dispersive component. And each unit and its neighbors are characterized by a charge distribution that covers its entire surface, with both positive and negative regions, that can interact in Coulombic fashion with one another. But of greater interest to some is the potential presence of more localized attractive forces, typically between individual atoms on neighboring molecules.

A classic example is the H-bond (HB) which might connect a proton donor AH group with a proton acceptor atom, commonly through its lone pair. The century-long study of the HB [1-9] has led to a solid understanding of a number of its properties: structural, spectroscopic, energetic, and so forth. One can make predictions as to the relative strengths of different sorts of HBs that might influence crystal structure, and even hazard rough guesses as to the strength of any one such individual bond. But there is far less quantitative information available regarding many other noncovalent bonding interactions such as π··π stacking, and the broad spectrum of σ and π-hole bonds that are currently under intense scrutiny. The latter include the halogen bond (XB) and a number of its close cousins such as chalcogen, pnicogen, and tetrel bonds which are only now beginning to be analyzed in a thorough manner [10-20].

A highly desirable goal would be the ability to dissect a crystal structure on the basis of the attractive forces holding the subunits together in a precise lattice. That is, what is the contribution of each noncovalent bond that might be present, HB, XB, π··π, or otherwise to the total pairwise interaction. From a purely crystallographic perspective one of the most common means of assessing the strength of a possible noncovalent bond between atoms on the two units is to compare the distance between them with the sum of their tabulated van der Waals radii. The premise of this idea is that as the bond between them strengthens, they will be drawn in closer together. It is thought that the ratio between this distance and Σr_{vdW}, sometimes referred to as the normalized contact distance, normalized distance parameter, or reduction ratio, offers a quantitative measure of the strength of this particular noncovalent bond. While offering an appealing opportunity to assess the bond strength through purely structural data, this measure is based more on intuition than on a solid theoretical footing.

The central goal then, the holy grail if you will, is to elucidate the strength of any one such specific interaction within the context of a pair of larger species. It is here that quantum chemistry can play a pivotal role. It is possible to design a replica of the crystal structure, and consider the interaction between a pair of molecules in a highly detailed manner. The energetics of binding of the two units can be easily calculated, but there is a great deal more information available via analysis of the wavefunction. Small modifications can be made in each subunit so

as to develop a database dealing with how different substituents affect the interaction. One can consider the sensitivity of the energetics to deviations from an ideal geometry in a systematic way.

However, as simple and straightforward as this may sound, the devil is truly in the details. This article is designed to outline the issues that can confound the application of quantum chemistry to elucidate the quantitative contribution of a given noncovalent bond to the accumulation of all components that go into the final structure adopted by the subunits within a crystal. It is hoped that the reader will thus gain a deeper appreciation of these issues and be better equipped to place quantum chemical information in its proper perspective.

GENERAL THEORETICAL FRAMEWORK

Reducing the problem to an oversimplified cartoon, one may be interested in the A--B interaction, indicated by the black double-arrow in Fig 1. This will typically be a point-to-point contact between a pair of atoms A and B. An example might be a OH··N H-bond or a CI··O halogen bond. Or the A and B moieties might be slightly larger as for example a pair of carbonyl C=O functional groups. An even larger example would be perhaps a pair of aromatic rings, parallel to one another in a π··π interaction.

The most widely used approach by quantum chemists to quantify the strength of the A··B interaction is to compute the interaction energy between the two constituent molecules 1 and 2, conceived as the purple dashed ovals in Fig 1. However, there are some obvious flaws in equating this interaction energy with the A··B bond. In the first place, the interaction energy will include not only the energetics of the A··B bond, but also any other specific bonds that might be present, suggested by the red dashed broken arrows between groups C and D or E and F. Like A··B, these would also be specific point-to-point interactions such as HBs or any other of that sort.

At first blush, it might be tempting to simply remove these other groups, replacing them by H or perhaps a larger nonpolar group such as methyl. Indeed, substitutions of this sort would certainly delete the C··D and E··F bonds from the picture. However, such a substitution ignores the effect that these various C, D, etc groups have on the A and B atoms of interest. As indicated by the blue curved arrows there is a certain amount of electron shift, i.e. inductive or polarization, that takes place within each subunit which would be changed, perhaps dramatically so, by the aforementioned replacement. Some schemes have been proposed that partially circumvent this problem by strategic design of closely related molecules, with and without the bonding groups, and then addition and subtraction of their total energies [21-29].

It is a common approach in dealing with noncovalent bonds to take the total interaction energy and dissect it into several components which conform to general ideas about interactions in general. There are numerous frameworks to accomplish this task [30-37], but they all share several general organizational concepts. The components of these schemes typically comprise first an electrostatic term which considers the charge distributions of the two subunits, and a steric repulsion between their electron clouds. Charge and polarization are usually lumped

together into an induction or orbital relaxation energy, and the final piece is the attractive dispersion energy. While this technique is quite useful in offering insights into the phenomena that play into the interaction, it suffers from the same issues as the total interaction energy itself. That is, the electrostatic term for example, would be that not only between A and B, but also involve the C··D and E··F pairs, as well as the charge distributions of the rest of each subunit.

While the replacements indicated above represent an attempt to delete other specific interactions between subunits 1 and 2, there remains the large question of nonspecific interactions. The wavy green lines in Fig 1 are meant to suggest the interactions that occur some distance from the A and B atoms of interest. The nature of this interaction can be quite varied. In the first place, each of the subunits would normally be characterized by a charge distribution, positive in some places and negative in others. These charge patterns would interact with one another, attractive in some places and repulsive in others, depending on the details. And this electrostatic energy would generally be substantial. It is emphasized that this Coulombic force is delocalized over the entire breadth of each of the two subunits, so cannot be associated with any one specific noncovalent bond.

Another attractive component would arise from dispersion, which would tend to grow along with the size and polarizability of each subunit. This attractive force is not confined in any sense to the particular bonding atoms of interest, but derives from the electron clouds that extend over the entire system. And of course there would be a certain amount of steric repulsion which would grow exponentially as the two subunits come close together. This overly close encounter may occur between the atoms of interest on the two subunits, or may arise at a location far removed from this reaction center. All of this is meant to stress that it would be a mistake to equate the total interaction energy between subunits 1 and 2 with the energy of a particular A··B component, even if the latter is likely to be sizable.

Analysis of Wavefunctions

Quantum mechanical procedures developed in recent years do offer a vehicle by which to home in one particular interaction amongst many. Quantum Theory of Atoms in Molecules (typically referred to by its abbreviated acronym AIM) analyzes the topology of the electron density of a system [38, 39] such as that pictured in Fig 1, and determines what are called bond paths that connect atoms that are presumed to be bound to one another, even if only weakly. In a case such as that in Fig 1, one would expect to see bond paths connecting A and B, as well as C--D and E--F. Further details about the bond path offer some quantitative estimates as to the strength of each bond, exclusive of the others. Most commonly used in this regard are the properties of the critical point located along the bond path. It is widely believed that the magnitude of the density at that point, the Laplacian of the density, or the potential energy density, are all closely correlated with the actual bond strength. Indeed, there are attempts in the literature [40-45] to apply a simple linear relation between a chosen bond critical point property and the full bond energy.

A typical example of some of these ideas is provided by a very recent study of a crystal containing perfluorinated iodo and bromobenzenes [46] and their interactions with Cu_4I_4 clusters

which are held together by CH··F and CH··Br HBs, I··Br XBs, and I··π contacts, amongst others. AIM analysis of segments of the clusters provided bond critical point parameters that were then related by an empirical relationship to estimate energies of each individual contact. However, it was deemed necessary to apply the same relationship to each sort of interaction, regardless of type. And the individual bond energies estimated in this manner seemed artificially low, summing to far less than that obtained for the total interaction energy.

There are other weaknesses in this approach. In the first place, the proposed correlations between actual bond energy and any particular AIM quantity have not proven reliable. Moreover, it appears that one would need a separate set of correlation parameters for each sort of interaction, whether H-bond (HB), halogen bond (XB), chalcogen bond (YB), lp··π, and so forth. As a perhaps more fundamental issue, there have been numerous examples presented in the literature where AIM bond paths failed to materialize even when noncovalent bonding is obvious, or a false positive was indicated wherein a bond path connects atoms which are clearly not attractive toward one another [47-55]. For example, a recent work has documented that even after two groups have been jammed much too close together, and their interaction has turned purely repulsive, that AIM indicates a bond that continues to grow stronger [56]. Another weakness of AIM is its ineffectiveness in identifying attractions between the π-systems of aromatic rings, which are not easily reduced to atom··atom. The reduced density gradient (RDG) approach is an offshoot of AIM which delineates regions in three-dimensional space whose level of attractiveness or repulsion is signaled by a particular color scheme. This method does appear to be a little better at identifying interactions such as π··π which do not track closely to an atom-to-atom bond picture. However, RDG also suffers from the weakness of misrepresenting close repulsive contacts as attractive [56].

Another means of analysis of the wave function also goes beyond overall general interactions, and opens a window into specific contacts. The Natural Bond Orbital (NBO) approach [57, 58] provides information about charge transfers between occupied and vacant orbitals of the two groups involved. Taking the AH··B H-bond as an example, NBO computes the amount of charge that is transferred from the lone pair of the nucleophilic B atom to the unoccupied σ*(AH) antibonding orbital of the proton donor. It is this transfer that has been identified as the principal source of the well known red shift of the A-H stretching frequency that occurs upon HB formation. The energetic consequence of this charge transfer provides a quantitative guide as to the strength of this HB, or in fact many other noncovalent bonds. As such, NBO provides a means of focusing on one particular bond, say A··B in Fig 1, exclusive of any others such as C··D or E··F. Some NBO quantities, particularly the second-order perturbation energy associated with the transfer in question, have found widespread application in estimating bond energies in HBs [59-61] and other noncovalent bonds [62-64].

Despite its usefulness, it is problematic to equate this NBO measure of charge transfer with the actual bond energy. In the first place, NBO concerns itself only with one element of the full interaction, viz the charge transfer energy. Secondly, it is not the full charge transfer, but rather a single element involving only one pair of orbitals. As another issue, if two groups are pushed too

close together, such that the steric repulsion takes hold and the interaction becomes purely repulsive as the total energy rises, NBO does not recognize this change [56]. The overly close contact raises the interorbital charge transfer, and this energetic component signals a continued stabilization, opposite to the full energy which is rising steeply. One might summarize this issue with NBO, as well as AIM, as follows. While they might be helpful in estimating bond energies of groups held apart beyond their equilibrium distances, both will fail to signal a repulsive potential if the groups are forced too closely together, and even suggest the interaction is growing more attractive.

Geometric Aspects

Another issue worthy of discussion relates to the geometry of the dyad chosen for study. At first blush, it would seem obvious that one ought to take the coordinates directly from the crystal structure, with or without a small amount of refinement. But it must be understood that the crystal structure results not only from the forces within the dyad of choice. There are numerous other forces present that account for the final geometry chosen. There are of course interactions with species that are not part of the dyad system. These external moieties not only interact directly with each subunit of the dyad but also modify their internal electronic structure, e.g. via polarization or charge transfer, so as to adjust the interaction present within the dyad itself. As one possible consequence, the geometry of the dyad, with all of its external influences, may push the species closer together than they would otherwise be. The structure of this crystal dyad may consequently lie on the repulsive wall of the potential energy surface, such that the interaction energy is reduced or even positive, i.e. repulsive. One might therefore arrive at the erroneous conclusion that the noncovalent bond of interest is overly weak, or even entirely absent. In reality, the bond is present, but requires the peripheral surrounding molecules to properly polarize the two interacting species to bring it to full fruition.

EXAMPLES

Example 1 - Anion··Anion Interactions

A particularly obvious example of some of these concepts arises in connection with the interactions between anions within the context of a crystal that of course also contains positive counterions. As one example, the polymeric structure of one particular crystal [65] places $(HgCl_3)^-$ anions in close proximity to one another, arranged in such a way that a Cl atom of one anion lies directly above the Hg of another, separated by 3.04 Å. A calculation of the interaction energy between these two anions at the M06-2X-def2TZVPP level in this particular alignment leads to a large positive value in a repulsive potential. One might thus be tempted to assume that there exists no noncovalent bonding between this pair.

However, a deeper analysis leads one to question this assumption. The particular mutual orientation allows more negative segments of one species to approach less negative areas of its neighbor, minimizing the anion-anion Coulombic repulsion. There is also suggestion of a noncovalent “spodium” bond in which charge migrates from the lone pair of the Cl of one anion

to the π-hole that lies above the Hg of its partner. These spodium bonds are indicated by both an NCI surface between the relevant groups and AIM Hg··Cl bond critical points with a density of 0.022 au, in the range normally expected for a noncovalent bond. But to reiterate, the interaction energy between these two anions is quite repulsive, +50 kcal/mol. One sees here an obvious case where both NCI and AIM suggest a bonding interaction despite a highly repulsive interaction.

Further probing brings out more subtle issues. When the geometry of this dyad of two $(HgCl_3)^-$ anions was allowed to adjust, these two anions moved further and further apart, not surprising in view of their negative charges. If however, this dyad system is placed within a polarizable continuum, a first crude approximation to the crystal environment, the two anions can approach one another to form a metastable minimum, which can be more stable than the separated species if the dielectric constant of the surrounding medium is large enough. And importantly, their equilibrium contact distance is 3.62 Å, much longer than that observed in the full crystal. So here, there would be little question of the existence of the purported Hg··Cl noncovalent bond so long as there is a polarizable medium and the intermolecular distance is long enough. If these two anions are jammed together to their crystal separation, the interaction is repulsive, even in the context of a high dielectric constant environment, so one might argue for the disappearance of this stabilizing bond.

The aforementioned example is not an isolated one. The $(HgCl_3)^-$ dimeric system above has been generalized to the spodium bonds of $(MX_3)^-$ where M can be Zn, Cd and Hg, with X representing Cl, Br, or I [66]. There is now a good deal of evidence that anions can in general interact with one another so as to form a metastable minimum, so long as there is a surrounding polarizable continuum to mitigate the ion-ion Coulombic repulsion [67-77]. Even when this complex is less stable than the pair of separated anions, the AIM parameters indicate the presence of a legitimate noncovalent bond [78], bringing to the fore the question as to whether a metastable equilibrium, higher in energy than the two isolated subunits, ought to be categorized as a stabilizing interaction. In a broader sense, it is possible to find exothermic binding between pairs of anions, but only under certain conditions [79]..

These ideas can be extended to explicitly consider neighboring units within the crystal. As one example, a survey of crystals containing the $(PdCl_4)^{2-}$ species identified numerous species similar to $(HgCl_3)^-$ where the Cl of one unit lies directly over the π-hole above Pd in another [80]. Again, the application of quantum calculations to the crystal separation demonstrated a strong native repulsion. Adding a pair of positive counterions to the system allowed the two anions to approach one another, reversing a repulsive potential to a strongly attractive one. A similar effect emerged if the actual $NH_3(CH_2)_6NH_2^+$ counterions were replaced by a constellation of point charges, mimicking the charges within the counterion itself. Both AIM and NBO treatments were successful in identifying interanion Pd··Cl bonds.

Amplifying on these ideas, a recent analysis [81] considered the structure of a crystal containing planar $(PdCl_4)^{2-}$ dianions, along with protonated diamine counterions, part of which is illustrated in Fig 2a. As in the system discussed above, Fig 2b shows how the lone pair of a Cl in the upper dianion approaches directly above the Pd of the lower unit. The geometry is conducive

to a noncovalent bond, as the Pd and Cl lie only 3.217 Å apart. Indeed, at the M06-2X/def2TZVPP level, AIM finds a bond path between Pd and Cl with ρ at the bond critical point of 0.014 au. Such a quantity would normally suggest the presence of a bond of significant strength. In strong contrast, however, the overall interaction energy between these two anions in their crystal structure is highly repulsive, by +212 kcal/mol. This system thus offers a glaring example where an AIM bond path may be misleading about the nature of the full interaction.

This repulsion abates, but only by a small amount, if 4 neutral species are placed in their vicinity, in the positions of the N atoms on the counterions in Fig 1b. On the other hand, if these four species are each positively charged, the interaction becomes attractive, and substantially so with the interaction energy roughly equal to 100 kcal/mol. Changing from four monocations to a pair of dications makes the interaction slightly more attractive, roughly 120 kcal/mol. It is worth stating that during this entire process of adding counterions, where the interaction reverses from strongly repulsive to highly attractive, the AIM bond critical point density remains completely static.

These anion··anion interactions thus provide a clear example of the issues arising in choosing a geometry to study. If one focuses on the crystal coordinates, various analysis modes can and do find evidence of specific noncovalent bonds. But at the same time, the intermolecular potential is quite strongly repulsive which would make the categorization of a noncovalent bond questionable. It is possible to reverse the situation to an attractive potential by the inclusion of additional species or an overall polarizable continuum environment, which would indeed suggest the presence of a stabilizing noncovalent bond. Even there however, the equilibrium intermolecular distance is somewhat longer than the crystal structure, and the potential might remain repulsive at the crystal separation.

These findings also bring up another and perhaps more philosophical question. In many ways these interactions between anions can be considered as a “normal” noncovalent bond, whether spodium or otherwise, layered over an overall stronger Coulombic repulsion between two ions of like charge. Indeed, there have been computations that bolster this view of these forces [82]. So an essential question emerges: Should a point-to-point attraction be considered as a true attraction that helps hold these ions together even though the total interaction between the two anions is a repulsive one? After all, this repulsion is weaker than would be the case if the noncovalent bond were absent.

Example 2 - Sn··P Tetrel Bond

These issues are not limited to charged species, but also plague the more common interactions between neutrals. One may take as an example, the cocrystal formed between $Sn(C_6H_5)_3Cl$ and triphenylphosphine. The two molecules line up within the crystal [83] in such a way that the P sits nearly directly along the Cl-Sn bond extension, with a R(Sn··P) separation of 3.541 Å, the configuration of a classical tetrel bond (TB), as may be seen in Fig 3a. The interaction energy of this pair was computed to be 14.40 kcal/mol at the M06-2X/def2-TZVP level. But does that mean that this quantity refers to the TB itself? This quantity is larger than

most tetrel bonds considered in the literature. And after all, there are other units present which might interact with one another. In principle, the three phenyl groups on each subunit might interact with one another, or with the Sn or P atoms on the partner subunit. AIM analysis of this structure in Fig 3b reveals six intermolecular bond paths, in addition to that connecting Sn with P. As compared to the density of 0.0113 au for the Sn··P bond path, the other six have magnitudes between 0.0039 and 0.0066, so consequently cannot be simply discounted, at least collectively.

What happens then if these six phenyl groups are all replaced by methyl? The latter are too far apart to interact directly with one another, as may be seen in Fig 3c. Making this substitution reduces the interaction energy to 8.78 kcal/mol [83]. Is this quantity a truer measure of the actual TB strength? After all, the methyl and phenyl groups are not too different in terms of electron-withdrawing capacity, so they ought not have too much influence on the charge patterns around the central Sn and P atoms. On the other hand, the smaller methyl group has less capacity for polarization, to shift density as the tetrel bond is being formed, which might reduce the strength of this TB. As one concrete manifestation of changes of the electronic structure of the Sn subunit, the replacement of its three phenyl groups by methyl reduces the depth of the σ-hole on the Sn from 43.2 to 19.2 kcal/mol. This rather drastic drop would play a major role in the lowering of the interaction energy that was observed so perhaps the methyl substitution does indeed represent an artificially low estimate of the TB energy.

With regard to AIM analysis, the diagram of the methylated dimer is displayed in Fig 1d. In addition to the desired Sn··P bond path, there is a second one connecting H atoms of two methyl groups. However, the density of this bond critical point is quite low. Moreover, such H··H paths are thought to represent an anomaly of the AIM treatment, and do not indicate any attractive binding. The density of the Sn··P bond critical point in the methylated dimer of Fig 1d is 0.0115 au, nearly identical to that in the more faithful triphenyl system, which might suggest that the interaction energy in the methyl model might comprise an accurate assessment of the TB energy. However, the literature would suggest that this density is more indicative of the distance between the two atoms than of the bond strength per se. And since this distance was held to be equal in the two cases, the equality of ρ might seem preordained.

Another means to extract the interaction energy of the Sn··P TB is via molecular tailoring, which deletes the interactions involving the phenyl groups in stepwise fashion. As explained in Fig 4, in addition to the full system (a) itself, one calculation (b) is performed to evaluate the energy of the same system but with the 3 phenyl groups on P replaced by H; likewise another (c) with the phenyls on Sn replaced by H. Finally, all phenyls are mutated to H in (d). Both b and c have removed the phenyl-phenyl interactions; moreover b has deleted the Sn··phenyl group interactions, and P··phenyl are removed in c. By subtracting the b+c energy sum from a+d, one arrives at an estimate of the pure Sn··P interaction energy in the absence of any other possible bonds. This quantity is computed to be 4.83 kcal/mol, again at the M06-2X-def2-TZVP level, certainly representing a substantial bond strength although significantly smaller than the

counterpoise-corrected interaction energy of 8.78 kcal/mol in the $ClMe_3Sn\cdot\cdot PMe_3$ complex or 14.40 kcal/mol for the larger phenylated dimer.

The value of 8.78 kcal/mol was extracted when the two subunits are held to the precise separation of 3.541 Å which occurs within the crystal. How much is this distance influenced by crystal packing forces? If left to their own devices, would these two subunits approach more closely, or are they pushed too close together in the crystal, and would prefer a greater separation? An optimization of the methylated $SnMe_3Cl\cdot\cdot PMe_3$ dimer led to a 0.25 Å closer approach to a distance of 3.290 Å. Allowing this shorter intermolecular separation slightly stabilizes the system by 0.56 kcal/mol to 9.34 kcal/mol, so while the crystal does appear to pull the two units apart, this stretch has only a small consequence for computing the TB energy.

The above discussion vividly illustrates the complexity of issues encountered when trying to elucidate the contribution of any one particular bond to the totality of forces holding units together within a crystal. The Sn··P TB energy was estimated to be 4.8 kcal/mol by molecular tailoring as the smallest estimate. A straight computation of the interaction energy when all phenyl groups have been replaced by non-interacting methyls, including full counterpoise correction is quite a bit larger at 8.8 kcal/mol, while the interaction energy of the full complex with six phenyl groups is 14.4 kcal/mol.

One is left with a central question as to whether this Sn··P TB is responsible for the structure of this cocrystal. Regardless of the specific means by which its energy is evaluated, it certainly represents a substantial contribution to the total interaction energy. Its energy is at least as large as a typical HB and there is little doubt expressed in the literature concerning the ability of HBs to direct crystal structure, even those much weaker than this TB. Closer scrutiny of the structure indicates that for the most part, the phenyl rings on the Sn are not aligned parallel to those on the P, thus minimizing any incipient π-π stacking forces which would compete with the TB. So at least as far as specific noncovalent bonds are concerned, it would certainly appear this TB is the dominant one.

Example 3- Types I and II Halogen Bonds

Another vivid example of some of these issues arises in the context of the interactions between halogen atoms. It has become axiomatic in the crystallographic literature that these interactions typically fall into one of two categories [84-86]. Type II as it is usually called is abbreviated simply as T2 in Fig 5 and fits the general criteria of a classic XB. θ_1 is roughly 180° so that the σ-hole generated by the R-X_1 bond points toward X_2 on the partner molecule. The other unit serves as electron donor and is oriented with θ_2 roughly equal to 110° so that one of its lone pairs points along the X··X axis and is optimally positioned to donate charge to the acceptor on the left. The second category, and another motif which is commonly observed within crystals, is designated at Type I, or T1. What is perhaps surprising is that the two θ angles are roughly equal to one another in this symmetric geometry. As such, neither has its σ-hole pointing directly at the other X atom, nor does either position its lone pair optimally for donation. T1 structures have not been observed as minima on the potential energy surface in numerous quantum

chemical calculations of XBs over the years, which is understandable in light of the angular deformations mentioned above. Despite these considerations, the T1 motif is quite a common one within crystals.

The large population of T1 structures within crystals thus poses some real questions. Does this sort of halogen bond represent a truly stable geometry in its own right, and if so, why is this motif not seen outside the province of crystals? Is this a geometry that owes its existence to crystal packing forces? If indeed a stable geometry, what forces might account for its low energy. How does the stability of T1 compare with its classical T2 cousin?

Quantum chemical calculations designed to address these questions [87] provided some insights into the stability of T1 as well as the source of its internal bonding. A set of small halogen fluorides were paired with one another as homo and heterodimers of HCl, HBr, and HI. In all cases, the T2 structure was found to represent a minimum on the surface at the M06-2X/aug-cc-pVTZ level while T1 could only be achieved if the two θ angles were forced to be equal to one another. In other words, there is in fact no T1 minimum for any of these systems. But importantly, the T1 structure was only slightly less stable than the T2 minimum. More specifically, Table 1 shows that the interaction energies within these dimers were in the range of 2-5 kcal/mol, and the T2-T1 energy difference was only about 1 kcal/mol, less than that in some cases.

Although not minima on the surface, vibrational analysis of these T1 structures revealed only a single imaginary frequency. The normal mode corresponding to this frequency represents a motion that interchanges the two molecules within the T2 minimum so that the electron donor becomes the acceptor and vice versa. The pathway for this interchange process is a narrow low energy corridor along the potential energy surface. The details of the geometry along this interconversion may be seen in Fig 6 for the particular example of FI··IF.

A central question concerns the nature of the binding within the T1 structure, since the mutual orientation has turned the σ-hole of one molecule from the other, and likewise for the lone pairs which are misaligned with the X··X axis. The calculations revealed that even in this distorted arrangement, the XB is only destabilized by a small degree. An added benefit of the symmetric T1 geometry is that there are two such XBs present, albeit both somewhat misaligned. The upshot is that the two distorted XBs add up to nearly as much stabilization as the single T2 XB, hence the fairly small T2 - T1 energy difference.

These results present several interesting conclusions regarding the observations of XBs within crystals. First of all, it is not only the pure T2 and fully symmetric T1 geometries that are of low energy. The entire corridor for the conversion from T2 to T1 is quite stable so would be prominently observed within crystals. One should therefore be careful about a designation scheme that defines a sharp boundary between the two: it would be more accurate to consider a gradual transition as the two molecules rotate, and a sort of blurry boundary.

As another issue, the results show that it is not necessary for a given dimer configuration to represent a true minimum in the gas phase in order for that structure to be prevalent within the confines of a crystal. T1 would not appear in a search for minima in any $RX_1\cdot\cdot X_2R$ dimer,

whether homo or heterodimer. Yet because of its low energy, even minor crystal packing considerations are sufficient for this sort of transition state geometry to occur quite commonly. And it would be a mistake to overlook its energetic contribution to the final crystal structure.

Example 4 - Types I and II Chalcogen Bonds

Given the basic similarities of halogen and chalcogen bonds, it is natural to inquire as to whether both T1 and T2 chalcogen bonding arrangements ought to occur, either in the gas phase or within a crystal. There has been little consideration given to this issue in the crystallography literature, so quantum calculations might offer some preview as to what to expect. A dataset was constructed [88] in which various chalcogen Y atoms were double-bonded to C in a formaldehyde-like motif. The two H atoms on the C were each in turn replaced by F so as to widen the spectrum of electron withdrawal from the Y atom.

This sort of system differs from the XB dimers in that each Y atom has two lone pairs instead of three, but again the σ-hole lies along the extension of the C-Y bond. The salient alignments are pictured in Fig 7 where the Y σ-hole is represented by the open shape containing a positive sign. The lone pair on its partner Y is designated by the filled shape with a negative sign. As in the XB systems, T2 again presents the optimal alignment of these two entities, whereas the symmetric T1 contains a significant misalignment, which is in part compensated by the presence of a second stabilizing, albeit bent, YB.

The actual geometries obtained by optimizations [88] are displayed in Fig 8, for the particular case of Y=Se; the T2 structures on the left, and the right side shows T1. As one progresses down the figure, the F substituents are gradually replaced by H. In some cases, these structures were true minima, while in others they could only be achieved by imposing some sort of geometrical restriction. For example, T1 required a restriction that the two CY··Y angles be held equal to one another, although this was unnecessary for some of the more strongly bound complexes. Some of the T2 geometries also required a restriction for certain pairs.

The interaction energies in these dimers calculated at the M06-2X/def2-TZVP level are listed in Table 2 where they may first be seen to be significantly smaller than the XB dimers in Table 1. These quantities span a range between less than 1 up to almost 3 kcal/mol. The AIM and NBO markers of these YBs are consistent with the weakness of these interactions. But again, with only one exception, T2 is more stable thanT1, even if only by a small amount. What does this mean for crystal environments? First, the small energetic differences between T1 and T2 ought to make these two sorts of geometry roughly equally preponderant. But also of importance, since these interaction energies are quite small, it would be a simple matter for crystal packing forces to derail these structures, pushing them toward geometries that are not consistent with these gas phase dimer calculations. Even if present these YBs would likely contribute only small amounts to the total binding forces.

The systems in Fig 8 insulate the Y atom from the full effect of the electron-withdrawing F atoms to some extent. When the C atom is removed, the smaller YFH molecules can engage in much stronger YBs. As exhibited in the last row of Table 3, the YBs formed by FYH which

contains a single F atom are even stronger than the XBs of the FX units in Table 1, with binding strengths between 4 and 10 kcal/mol. Note however, the interesting reversal in stability in that T1 is lower in energy than is T2. In fact, T2 is not even a minimum on the surface of these homodimers, and appears only if the electron donor atom is restricted to the FY axis. In any case, the substantial magnitudes of the interaction energies of these systems suggest the presence of an electron-withdrawing substituent on the chalcogen atom ought to manifest itself in YBs within the context of crystals. One would anticipate a slight preference for symmetric Type I geometries, but less symmetric T2 forms would also be present to a significant degree.

Example 5- Segment Size

In modeling a crystal, there is the perennial issue as to how large a segment to consider. It is tempting to focus on a particular dyad as that which contains the particular noncovalent bond of interest. But in many cases, this small segment will ignore a score of other interactions which have some effect on the one of interest. It was shown earlier how adding counterions can drastically modify the nature of the interaction between anions. Even if an extended segment is chosen for study, there remains the issue of what geometry to examine. In other words, how well does a geometry optimization of this segment compare with the actual crystal structure?

A recent study attacked this question in particular [89] taking as its base the crystal structure of AsF_3 [90]. Fig 9a focuses on the structure of one central AsF_3 unit and its eight immediately surrounding neighbors within the crystal. The broken blue lines indicate the placement of intermolecular bond paths that involve the central unit, as interpreted by AIM analysis at the PBE0-D3/def2-TZVP level, and include numerous direct As··F ZB interactions. If instead of adopting the structure of this nonamer directly from the crystal, the geometry were to be fully optimized from first principles, the very different structure in Fig 9b is obtained. In order to understand the reason for this different shape, the total interaction in each cluster was partitioned into pairwise interaction energies for each pair of molecules. The first row of Table 3 shows that the sum of these pairwise energies that involve the central unit are fairly similar for the two geometries, 13.9 vs 15.8 kcal/mol. However, the total pairwise interaction sum involving only peripheral units is drastically different. The rearrangement from the crystal to the optimized structure increases this term sixfold from 6 to 36 kcal/mol.

In summary, the crystal segment and a like-sized optimized cluster are similar in terms of the binding energy of a central molecule to its neighbors. So it is reasonable to conclude that the various units in a crystal are well disposed to form strong ZBs to a central molecule. The difference arises in the comparison of the bonding of the peripheral molecules with one another. In the cluster, these peripheral units have an incentive to engage in strong ZBs with one another as a means of stabilizing the entire system, and they adjust their positions accordingly. In a crystal, by contrast, the peripheral molecules have an alternative. Instead of bonding strongly with another neighbor of the central unit, they can bind with other molecules in the crystal, those that are more distant from the central unit, not included within the nonamer, or in any cluster of

comparable size. This principle helps account for differences between the internal geometry of any given cluster and what is observed in a crystal.

Another major issue falls under the rubric of cooperativity. It is because of this phenomenon that a chain of *n* H-bonded water molecules is bound more tightly than n times the energy of the H-bond energy of a single isolated dimer. This same principle applies to other noncovalent bonds as well, such that it is favorable for a central molecule to play the simultaneous role of both electron donor and acceptor [91-98], as compared to acting as either double donor or acceptor. As an example of the latter negative or anticooperativity, each new pnicogen bond formed to a central ZF_3 unit (Z=P,As,Sb,Bi) becomes progressively weaker [78] which will have repercussions for the crystal structure ultimately adopted. This cooperativity can also operate when two adjacent atoms on a given molecule each act in a different capacity. That is, in a square $(YN)_2$ motif, each chalcogen (Y) atom acts as electron donor, and its neighboring N as acceptor, such that the two Y··N chalcogen bonds reinforce one another [99].

SUMMARY AND PROSPECTUS

It may be clear from the above that it is a straightforward matter to evaluate the energetics of the interaction between any pair of molecules. This task can be accomplished not only by a direct evaluation of the interaction energy itself, but there are also indirect measures that can be invoked via analysis of the wavefunction. But the real questions are deeper, almost philosophical. In the first place, what is the contribution of any one specific type of contact to the overall intermolecular interaction which typically comprises not only additional specific contacts, but also nonspecific stabilizations that might spread over the entire expanse of each unit, such as Coulombic forces and dispersion. Secondly, which species should be included other than the two molecules of particular interest?

In the first example described above, we have seen how the consideration of a pair of anions at their crystal separation offers a highly repulsive potential, even in the face of quantum chemical markers of a favorable interaction. However, this short-range repulsion can turn attractive by the introduction of several surrounding species such as counterions, or even a general polarizable continuum. But even then, the two anions would choose to lie further apart than in the actual crystal.

A related issue that begs further inquiry is the question as to how to dissect the total interaction energy into all of its component parts, only one of which involves the noncovalent bond of interest. The total interaction energy within a complex containing a Sn··P tetrel bond within a crystal also contained attractive elements involving peripheral groups such as phenyl rings. Different means of separating these components from one another did not all give consistent results with one another. And here is a case where the separation within the crystal is now *longer* than the optimal distance of the two units involved.

The crystallographic classification of X··X halogen bonds into Types I and II provided an example of how a particular configuration that does not represent a true minimum on the potential energy surface can nevertheless masquerade as one. That is, because Type I is only

slightly higher in energy than is Type II, and because their interconversion encounters no energy barrier, even weak crystal packing forces can be sufficient to result in numerous observations of Type I, as well as others that lie along the transition path between the two structures. When these ideas are extended to chalcogen bonds, the energies of Types I and II remain quite similar in most cases, such that both sorts can be expected within crystals.

The fifth case study above highlighted the sensitivity of the quantum calculation of the preferred geometry to the particular number of surrounding species. Even if considering all of the nearest neighbors to a pnicogen-bonded pair, and even a second shell of surrounding molecules, geometry optimization of the cluster can be fundamentally different than that within a full crystal, even if the specific interaction energies to the central pair of units are similar in the two cases.

In a more general sense, there is the question as to which intermolecular distance offers a better perspective on the contribution of the bond in question? The crystal distance might be much closer (or further) than the optimized geometry, so may not reflect the full potential of this bond to influence the structure. As a perhaps even more fundamental question, how does the strength of the interaction (assuming it could be calculated in a nonarbitrary manner) relate to its ability to affect a crystal structure? Of course, there would be little question that a very strong attractive force can dominate the assembly within a crystal. But on the other end of the spectrum are very weak bonds whose influence ought to be questionable. But can they exert a significant influence, weakness notwithstanding? A good example emerges in the interactions between methyl groups. A recent study combining a crystal structure survey with quantum calculations [100] found that in principle two methyl groups might approach one another, and that a very weak tetrel bond might form under the right conditions of selected substituents. However, these bond energies are exceedingly weak, only on the order of 1 kcal/mol or so. Despite this weakness, the survey of crystals in the literature noted that these bonds seemed capable of pushing the two methyl groups toward a mutual collinear orientation where they might engage properly, again even though the C··C contact distance was barely less than their vdW radius sum.

It is hoped that future researchers will tackle these questions head-on, and that quantum chemistry will be better positioned to answer questions concerning noncovalent interactions that are of greatest import to the field of crystallography.

Acknowledgements

This material is based upon work supported by the National Science Foundation under Grant No. 1954310.

Conflict of Interest

The author declares no conflict of interest.

REFERENCES

1. G. C. Pimentel and A. L. McClellan, *The Hydrogen Bond*, Freeman, San Francisco, 1960.
2. M. D. Joesten and L. J. Schaad, *Hydrogen Bonding*, Marcel Dekker, New York, 1974.

3. P. Schuster, G. Zundel and C. Sandorfy, *The Hydrogen Bond. Recent Developments in Theory and Experiments*, North-Holland Publishing Co., Amsterdam, 1976.
4. G. A. Jeffrey and W. Saenger, *Hydrogen Bonding in Biological Structures*, Springer-Verlag, Berlin, 1991.
5. S. Scheiner, *Hydrogen Bonding. A Theoretical Perspective*, Oxford University Press, New York, 1997.
6. G. Gilli and P. Gilli, *The Nature of the Hydrogen Bond*, Oxford University Press, Oxford, UK, 2009.
7. M. M. Szczesniak and S. Scheiner, *J. Chem. Phys.*, 1982, 77, 4586-4593.
8. M. M. Szczesniak, S. Scheiner and Y. Bouteiller, *J. Chem. Phys.*, 1984, 81, 5024-5030.
9. M. Cuma, S. Scheiner and T. Kar, *J. Mol. Struct. (Theochem)*, 1999, 467, 37-49.
10. I. Alkorta, J. Elguero and J. M. Oliva-Enrich, *Materials*, 2020, 13, 2163.
11. J. E. Del Bene, I. Alkorta and J. Elguero, *Chem. Phys. Lett.*, 2017, 685, 338-343.
12. I. Benito, R. M. Gomila and A. Frontera, *CrystEngComm*, 2022, 24, 4440-4446.
13. D. F. Mertsalov, R. M. Gomila, V. P. Zaytsev, M. S. Grigoriev, E. V. Nikitina, F. I. Zubkov and A. Frontera, *Cryst.*, 2021, 11, 1406.
14. V. Kumar, P. Scilabra, P. Politzer, G. Terraneo, A. Daolio, F. Fernandez-Palacio, J. S. Murray and G. Resnati, *Cryst. Growth Des.*, 2021, 21, 642-652.
15. P. Politzer and J. S. Murray, in *Noncovalent Forces*, ed. S. Scheiner, Springer, Dordrecht, Netherlands, 2015, vol. 19, pp. 357-389.
16. S. J. Grabowski, *Cryst.*, 2022, 12, 112.
17. S. J. Grabowski, *Phys. Chem. Chem. Phys.*, 2014, 16, 1824-1834.
18. L. M. Azofra and S. Scheiner, *J. Chem. Phys.*, 2015, 142, 034307.
19. G. Chalasinski, S. M. Cybulski, M. M. Szczesniak and S. Scheiner, *J. Chem. Phys.*, 1989, 91, 7809-7817.
20. Z. Latajka and S. Scheiner, *J. Chem. Phys.*, 1986, 84, 341-347.
21. M. M. Deshmukh, S. R. Gadre and L. J. Bartolotti, *J. Phys. Chem. A*, 2006, 110, 12519-12523.
22. M. M. Deshmukh and S. R. Gadre, *J. Phys. Chem. A*, 2009, 113, 7927-7932.
23. V. Singh, I. Ibnusaud, S. R. Gadre and M. M. Deshmukh, *New J. Chem.*, 2020, 44, 5841-5849.
24. D. Rusinska-Roszak, *J. Phys. Chem. A*, 2015, 119, 3674-3687.
25. M. Jabłoński, *Molecules*, 2020, 25, 5512.
26. G. Sanchez-Sanz, C. Trujillo, I. Alkorta and J. Elguero, *Phys. Chem. Chem. Phys.*, 2014, 16, 15900-15909.
27. J. N. Woodford, *J. Phys. Chem. A*, 2007, 111, 8519-8530.
28. I. Rozas, I. Alkorta and J. Elguero, *J. Phys. Chem. A*, 2001, 105, 10462-10467.
29. M. B. Ahirwar and M. M. Deshmukh, *J. Phys. Chem. A*, 2023, 127, 1219-1232.
30. K. Kitaura and K. Morokuma, *Int. J. Quantum Chem.*, 1976, 10, 325-340.
31. E. D. Glendening, *J. Am. Chem. Soc.*, 1996, 118, 2473-2482.
32. K. Szalewicz and B. Jeziorski, in *Molecular Interactions. From Van der Waals to Strongly Bound Complexes*, ed. S. Scheiner, Wiley, New York, 1997, pp. 3-43.
33. R. Z. Khaliullin, E. A. Cobar, R. C. Lochan, A. T. Bell and M. Head-Gordon, *J. Phys. Chem. A*, 2007, 111, 8753 - 8765.
34. P. Su and H. Li, *J. Chem. Phys.*, 2009, 131, 014102.
35. I. Mayer, *Phys. Chem. Chem. Phys.*, 2012, 14, 337-344.

36. C. D. Sherrill, *Acc. Chem. Res.*, 2013, 46, 1020-1028.
37. P. R. Horn, Y. Mao and M. Head-Gordon, *Phys. Chem. Chem. Phys.*, 2016, 18, 23067-23079.
38. R. F. W. Bader, *Atoms in Molecules, A Quantum Theory*, Clarendon Press, Oxford, 1990.
39. R. F. W. Bader, M. T. Carroll, J. R. Cheeseman and C. Chang, *J. Am. Chem. Soc.*, 1987, 109, 7968-7979.
40. E. Espinosa, E. Molins and C. Lecomte, *Chem. Phys. Lett.*, 1998, 285, 170-173.
41. I. Mata, I. Alkorta, E. Espinosa and E. Molins, *Chem. Phys. Lett.*, 2011, 507, 185-189.
42. E. V. Bartashevich and V. G. Tsirelson, *Russ. Chem. Rev.*, 2014, 83, 1181-1203.
43. M. L. Kuznetsov, *Molecules*, 2021, 26, 2083.
44. N. Kumar, S. Saha and G. N. Sastry, *Phys. Chem. Chem. Phys.*, 2021, 23, 8478-8488.
45. S. J. Grabowski, *Molecules*, 2020, 25, 4668.
46. Y. N. Toikka, G. L. Starova, V. V. Suslonov, R. M. Gomila, A. Frontera, V. Y. Kukushkin and N. A. Bokach, *Cryst. Growth Des.*, 2023, 23, 5194-5203.
47. R. Taylor, *CrystEngComm*, 2020, 22, 7145-7151.
48. M. Jabłoński, *Chem. Phys. Lett.*, 2020, 759, 137946.
49. A. Forni, D. Franchini, F. Dapiaggi, S. Pieraccini, M. Sironi, P. Scilabra, T. Pilati, K. I. Petko, G. Resnati and Y. L. Yagupolkii, *Cryst. Growth Des.*, 2019, 19, 1621-1631.
50. M. Jabłoński, *ChemistryOpen*, 2019, 8, 497-507.
51. C. R. Wick and T. Clark, *J. Mol. Model.*, 2018, 24, 142.
52. T. Clark, J. S. Murray and P. Politzer, *Phys. Chem. Chem. Phys.*, 2018, 20, 30076-30082.
53. D. Myburgh, S. von Berg and J. Dillen, *J. Comput. Chem.*, 2018, 39, 2273-2282.
54. S. Shahbazian, *Chem. Eur. J.*, 2018, 24, 5401-5405.
55. M. A. Spackman, *Cryst. Growth Des.*, 2015, 15, 5624-5628.
56. S. Scheiner, *J. Comput. Chem.*, 2022, 43, 1814-1824.
57. A. E. Reed and F. Weinhold, *J. Chem. Phys.*, 1983, 78, 4066-4073.
58. A. E. Reed, F. Weinhold, L. A. Curtiss and D. J. Pochatko, *J. Chem. Phys.*, 1986, 84, 5687-5705.
59. K. Wendler, J. Thar, S. Zahn and B. Kirchner, *J. Phys. Chem. A*, 2010, 114, 9529-9536.
60. V. Brenner, E. Gloaguen and M. Mons, *Phys. Chem. Chem. Phys.*, 2019, 21, 24601-24619.
61. A. M. Lamsabhi, O. Mó and M. Yáñez, *Molecules*, 2021, 26, 3556.
62. Y. Jiao and F. Weinhold, *Molecules*, 2019, 24, 2090.
63. S. Hayashi, M. Uegaito, T. Nishide, E. Tanaka, W. Nakanishi, T. Sasamori, N. Tokitoh and M. Minoura, *New J. Chem.*, 2019, 43, 14224-14237.
64. A. Gholipour, S. Farhadi and R. S. Neyband, *Struct. Chem.*, 2016, 27, 1543-1551.
65. R. Wysokiński, W. Zierkiewicz, M. Michalczyk and S. Scheiner, *ChemPhysChem.*, 2021, 22, 818-821.
66. R. Wysokiński, W. Zierkiewicz, M. Michalczyk and S. Scheiner, *Phys. Chem. Chem. Phys.*, 2021, 23, 13853-13861.
67. J. Li, Q. Feng, C. Wang and Y. Mo, *Phys. Chem. Chem. Phys.*, 2023, 25, 15371-15381.
68. L. Andreo, R. M. Gomila, E. Priola, A. Giordana, S. Pantaleone, E. Diana, G. Mahmoudi and A. Frontera, *Cryst. Growth Des.*, 2022, 22, 6539-6544.
69. M. Calabrese, A. Pizzi, A. Daolio, A. Frontera and G. Resnati, *Chem. Commun.*, 2022, 58, 9274-9277.
70. D. Fan, L. Chen, C. Wang, S. Yin and Y. Mo, *J. Chem. Phys.*, 2021, 155, 234302.

71. R. Wysokiński, W. Zierkiewicz, M. Michalczyk and S. Scheiner, *ChemPhysChem.*, 2020, 21, 1119-1125.
72. J. M. Holthoff, R. Weiss, S. V. Rosokha and S. M. Huber, *Chem. Eur. J.*, 2021, 27, 16530-16542.
73. A. Daolio, A. Pizzi, G. Terraneo, A. Frontera and G. Resnati, *ChemPhysChem.*, 2021, 22, 2281-2285.
74. C. Loy, J. M. Holthoff, R. Weiss, S. M. Huber and S. V. Rosokha, *Chem. Sci.*, 2021, 12, 8246-8251.
75. R. Wysokiński, M. Michalczyk, W. Zierkiewicz and S. Scheiner, *Phys. Chem. Chem. Phys.*, 2021, 23, 4818-4828.
76. Y. Li, L. Meng and Y. Zeng, *ChemPlusChem*, 2021, 86, 232-240.
77. D. Quiñonero, I. Alkorta and J. Elguero, *ChemPhysChem.*, 2020, 21, 1597-1607.
78. R. Wysokiński, W. Zierkiewicz, M. Michalczyk and S. Scheiner, *J. Phys. Chem. A*, 2020, 124, 2046-2056.
79. S. Scheiner, *Phys. Chem. Chem. Phys.*, 2022, 24, 6964-6972.
80. W. Zierkiewicz, M. Michalczyk, T. Maris, R. Wysokiński and S. Scheiner, *Chem. Commun.*, 2021, 57, 13305-13308.
81. R. Wysokiński, W. Zierkiewicz, M. Michalczyk, T. Maris and S. Scheiner, *Molecules*, 2022, 27, 2144.
82. I. Mata, I. Alkorta, E. Molins and E. Espinosa, *ChemPhysChem.*, 2012, 13, 1421-1424.
83. S. Liyanage, J. S. Ovens, S. Scheiner and D. L. Bryce, *Chem. Commun.*, 2023, 59, 9001-9004.
84. G. R. Desiraju and R. Parthasarathy, *J. Am. Chem. Soc.*, 1989, 111, 8725-8726.
85. V. R. Pedireddi, D. S. Reddy, B. S. Goud, D. C. Craig, A. D. Rae and G. R. Desiraju, *J. Chem. Soc. Perkin Trans. 2*, 1994, DOI: 10.1039/P29940002353, 2353-2360.
86. M. Fourmigué, *Curr. Op. Solid State Mat. Sci.*, 2009, 13, 36-45.
87. S. Scheiner, *Cryst. Growth Des.*, 2022, 22, 2692-2702.
88. S. Scheiner, *Cryst.*, 2023, 13, 766.
89. S. Scheiner, M. Michalczyk and W. Zierkiewicz, *Molecules*, 2022, 27, 6486.
90. A. Varadwaj, P. R. Varadwaj, H. M. Marques and K. Yamashita, *Molecules*, 2022, 27, 3421.
91. U. Adhikari and S. Scheiner, *J. Chem. Phys.*, 2011, 135, 184306.
92. X. Hui-Li, L. Qing-Zhong and S. Steve, *ChemPhysChem.*, 2018, 19, 1456-1464.
93. S. Scheiner, *Inorg. Chem.*, 2020, 59, 9315-9324.
94. N. Liu, X. Xie, Q. Li and S. Scheiner, *ChemPhysChem.*, 2021, 22, 2305-2312.
95. Y. Wei, Q. Li and S. Scheiner, *ChemPhysChem.*, 2018, 19, 736-743.
96. S. Scheiner, *J. Phys. Chem. A*, 2021, 125, 2631-2641.
97. Q. Yang, B. Zhou, Q. Li and S. Scheiner, *ChemPhysChem.*, 2021, 22, 481-487.
98. S. Scheiner, *J. Phys. Chem. A*, 2022, 126, 6443-6455.
99. S. Scheiner, *J. Phys. Chem. A*, 2022, 126, 1194-1203.
100. N. Keshtkar, O. Loveday, V. Polo and J. Echeverría, *Cryst. Growth Des.*, 2023, 23, 5112-5116.

Table 1. Interaction energies -E_{int} (kcal/mol) of indicated $FX_1 \cdot\cdot X_2F$ dimers[a]

$X_1 \cdots X_2$	T2	T1	T1 - T2[b]
I··I	5.19	4.71	0.48
Br··Br	3.04	2.10	0.94
Cl··Cl	1.73	0.98	0.75
I··Br	4.16	3.14	1.02
Br··I	3.84	3.14	0.70
Br··Cl	2.53	1.44	1.09
Cl··Br	2.04	1.44	0.60
I··Cl	3.50	2.14	1.36
Cl··I	2.59	2.14	0.45

[a]atom listed on left refers to electron acceptor

[b]energy of T1 relative to more stable T2

Table 2. Interaction energies, -E_{int} (kcal/mol), in homodimers

	S		Se		Te	
	T2	T1	T2	T1	T2	T1
YCF_2	0.82	0.43	1.13	0.74	2.44	1.70
YCHF	0.69	0.39	0.99	0.61	1.31	1.23
YCH_2	1.29	0.78	1.65	1.56	2.29	2.68
YFH	4.17	5.18	5.58	7.18	8.08	10.21

Table 3. Sums of pairwise interaction energies (kcal/mol) in nonamer of AsF_3

	crystal	cluster
Σc-p[a]	13.92	15.78
Σp-p	6.22	35.67
all pairs (sum of c-p and p-p)	20.14	51.45
actual E_{int}	19.98	54.87

[a]c – central unit, p – peripheral units

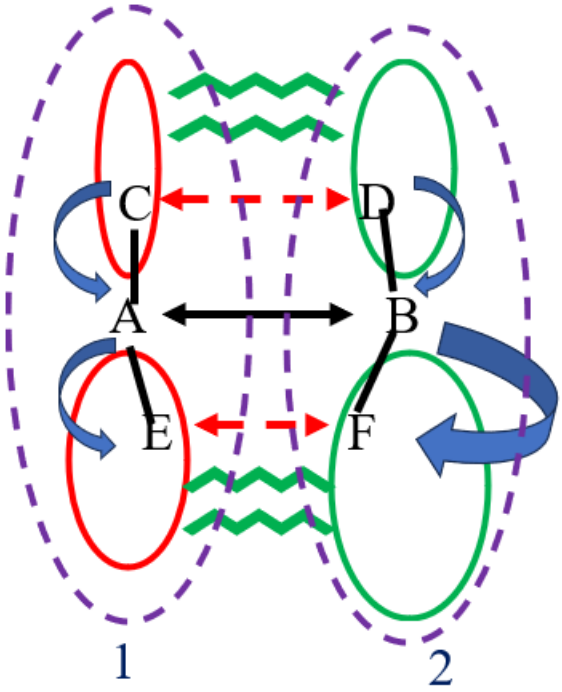

Fig 1. Schematic diagram of two interacting molecules, with specific contacts signified by double arrows, and nonspecific delocalized interactions by wavy lines. Curved arrows represent internal polarizations.

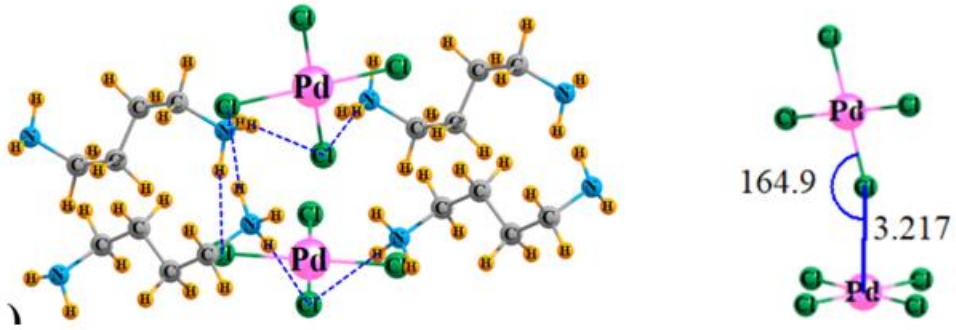

Fig 2. Interactions between $Pd(Cl_4)^{2-}$ dianions a) along with four protonated diamine counterions, b) specific Pd··Cl contact geometry. Distance in Å, angle in degs.

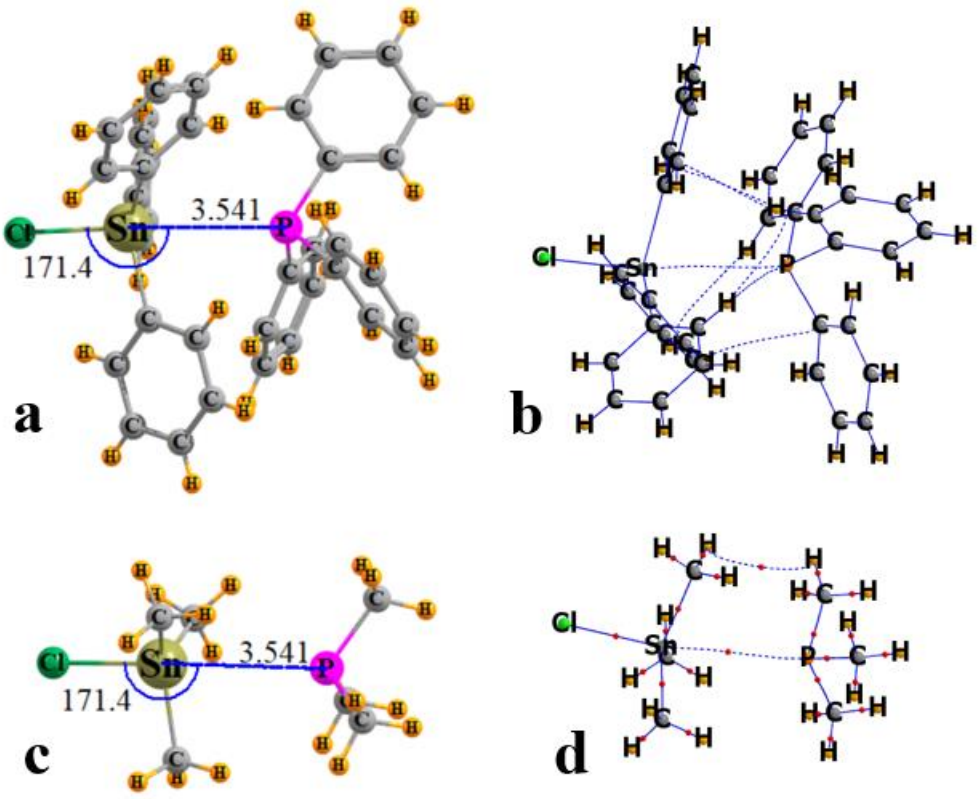

Fig 3. a) Geometry of cocrystal formed between $Sn(C_6H_5)_3Cl$ and triphenylphosphine, b) AIM molecular diagram showing intermolecular bond paths as dotted blue lines. c) Model with all phenyl groups replaced by CH3, and d) AIM diagram of this reduced model. Distance in Å, angle in degs.

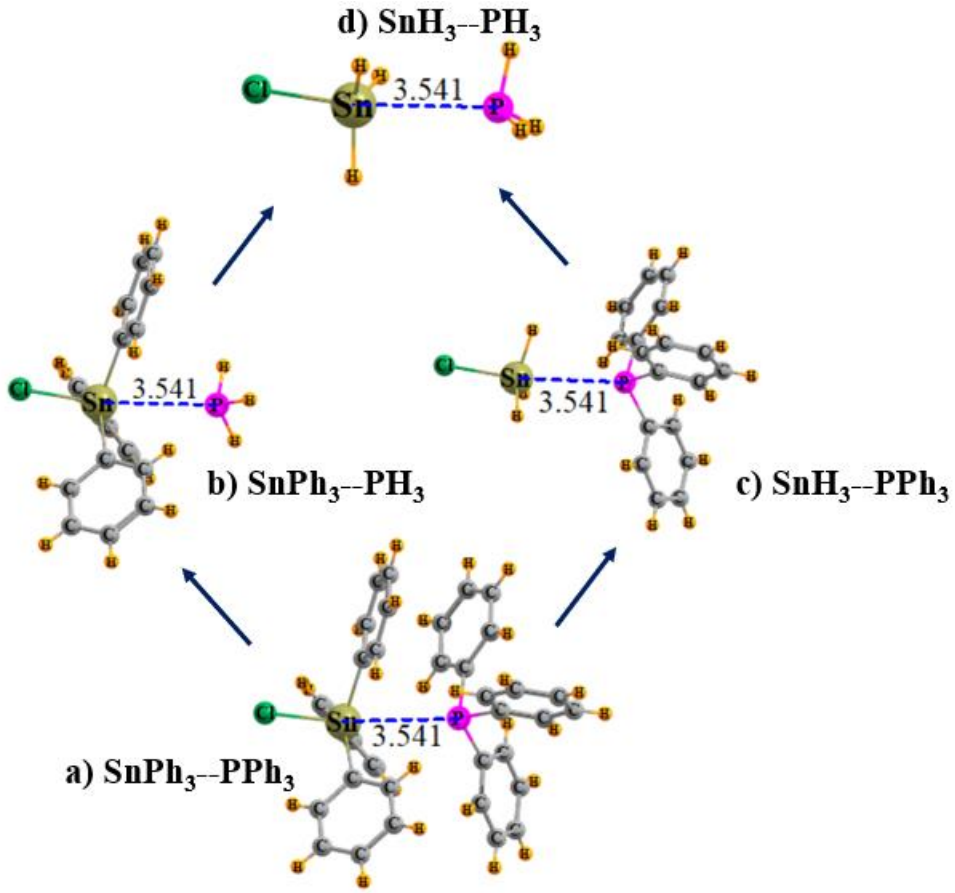

Fig 4. Molecular tailoring applied to estimate energy of Sn··P tetrel bond. Distances in Å.

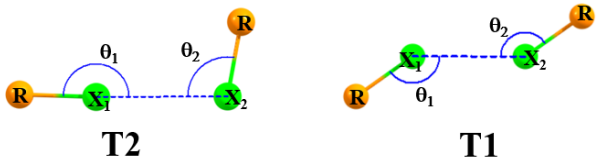

Fig 5. Definition of two types of X··X halogen bonds

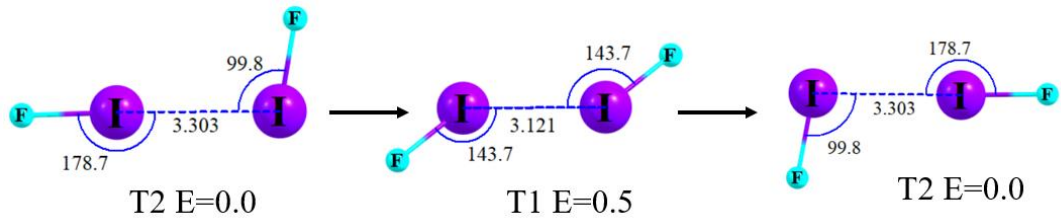

Fig 6. Pathway converting T2 to its mirror image, passing through T1 as a transition state. Distances in Å, angles in degs, energies in kcal/mol.

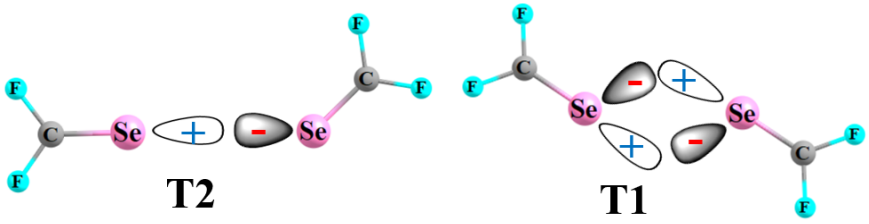

Fig 7. T2 and T1 Geometries of chalcogen-bonded CF_2Se homodimers

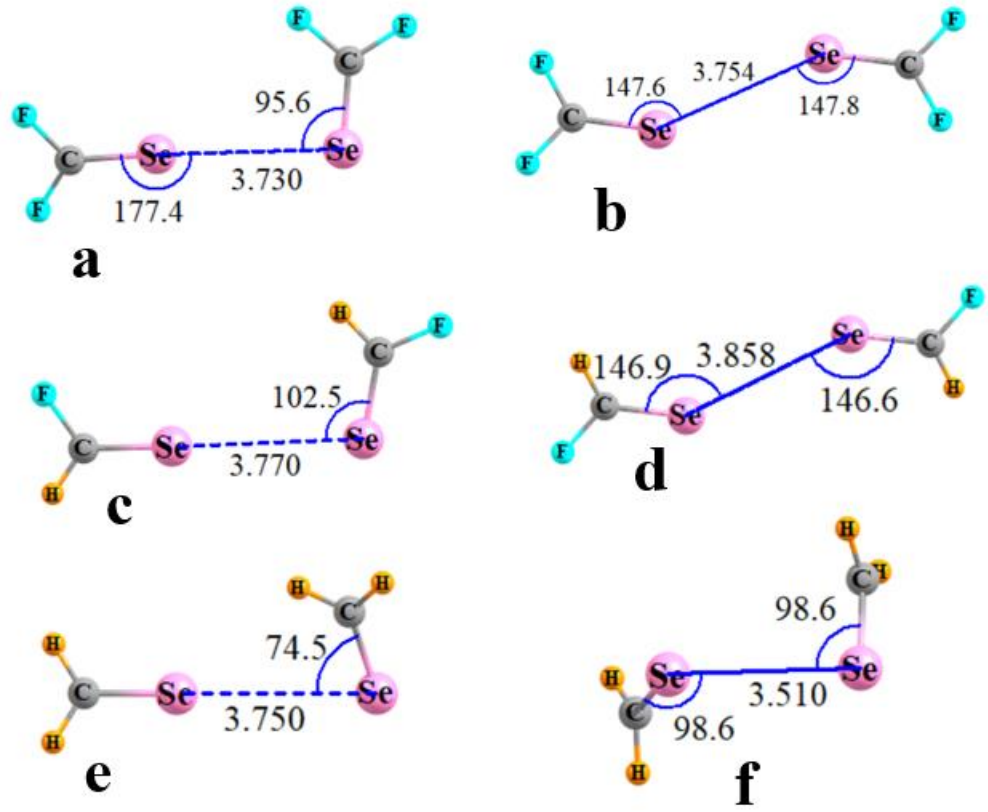

Fig 8. Optimized T2 (left) and T1 (right) geometries of chalcogen-bonded (a,b) CF_2Se, (c,d) CHFSe, and (e,f) CH_2Se homodimers. Distances in Å, angles in degs,

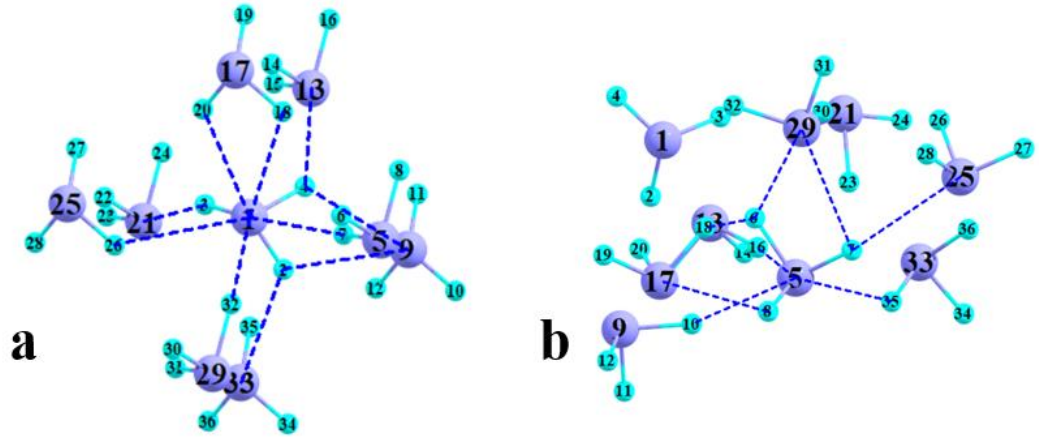

Fig 9. Geometries of nonamer taken from a) X-ray structure of crystal and b) optimization. Light blue refers to F atoms and As shown in purple. Dashed lines indicate AIM bond paths involving central AsF_3 unit.